AR-009-426

DSTO-TR-0273

# Initiation of Detonation in Composition B by an Underwater Shock Wave

Michael Chung,
Darren McQueen and
Lyn McVay



DEPARTMENT OF DEFENCE
DEFENCE SCIENCE AND TECHNOLOGY ORGANISATION

Mar-20

# Initiation of Detonation in Composition B by an Underwater Shock Wave

*Michael Chung, Darren McQueen and Lyn McVay*

**Weapons Systems Division**
**Aeronautical and Maritime Research Laboratory**

DSTO-TR-0273

**ABSTRACT**

This paper examines the interaction of underwater shock waves with bare, cylindrical Composition B acceptor charges. Suitable methods to discern detonation and non-detonation of an underwater charge were determined. Separation distances for the 50% probability of sympathetic detonation of Composition B acceptors using 0.5, 2.5, 5.0 and 10.0 kg spherical pentolite donor charges were calculated from the Bruceton technique. The variation in near-field shock wave velocity between donor and acceptor charges was modelled in terms of reduced charge separation to permit an economy of effort in predictions of the effects from underwater charges of a changed scale. Measurement of shock wave transit times indicate that initiation of detonation in the acceptor is due to the underwater shock wave alone.



DEPARTMENT OF DEFENCE

DEFENCE SCIENCE AND TECHNOLOGY ORGANISATION

*Published by*

*DSTO Aeronautical and Maritime Research Laboratory*
*PO Box 4331*
*Melbourne Victoria 3001*

*Telephone: (03) 9626 8111*
*Fax: (03) 9626 8999*

*AR No. AR-009-426*
*September 1996*

**APPROVED FOR PUBLIC RELEASE**

# Initiation of Detonation in Composition B by an Underwater Shock Wave

## Executive Summary

Current Navy operational doctrine recommends that the clearance of an under-sea ground mine is to be achieved by detonating the mine.

The most common method used to meet this requirement is the deployment of a large clearing charge placed either close by or in contact with the ground mine. Depending on the stand-off distance, the shock wave from the clearing charge may or may not initiate sympathetic detonation in the ground mine.

Although this method has been in service for many years, the critical initiation parameters of an underwater shock wave are not known. Consequently, predictive models are not available to assist Navy in the development of operational doctrine on clearing charge deployment.

This paper commences a study to investigate the critical initiation parameters of an underwater shock wave. The planned outcome of which, is to provide Navy with a simple analytical model to predict stand-off distances to sympathetically detonate a range of threat mines.

This paper describes a series of experiments that have determined the stand-off distances to achieve 50% probability of detonation of bare Composition B receptor charges. These distances have been determined for 0.5, 2.5, 5.0 and 10.0 kg pentolite donor charges. In the course of events, two techniques were developed to determine the type of event initiated by an underwater shock wave. One used contact witness plates and the other measured shock wave transit times. The measurements of shock wave transit times have also indicated that the initiation of detonation in the receptor is due to the underwater shock wave alone.

Measurements of the velocity of the underwater shock wave in the near field show that its velocity is very much greater than the acoustic velocity, resulting in underwater pressures being greater than those predicted by the similitude equations. Further experiments with shielded and encased receptors are planned to assist in determining the effect the casing of the sea-mine may have on the initiating parameters of an underwater shock wave.

# Authors

## Michael Chung
Weapons Systems Division

*Michael Chung joined DSTO in 1969 and has worked widely in the fields of Applied Physics at AMRL. Recent work has investigated the effects produced by the interaction of underwater shock waves with explosive materials and simple structures. He is an Associate of the School of Mines Ballarat and graduated from the Royal Melbourne Institute of Technology in Applied Physics.*

## Darren McQueen
Weapons Systems Division

*Darren McQueen completed the Certificates of Technology in Applied Mechanics and Mechanical Design Drafting in 1987, following his time as a Fitter and Machinist. He joined AMRL in 1987 and has worked on investigations into the effectiveness of explosive filled ordnance and explosively formed projectiles for low order disposal techniques.*

## Lyn McVay
Weapons Systems Division

*Lyn McVay graduated Bachelor of Applied Science in Chemistry from Victoria University of Technology in 1991. She commenced work at AMRL in 1986 and has recently worked on techniques to demonstrate low order explosive ordnance disposal and the effects of underwater sympathetic detonation.*

# Contents

# 1. Introduction

The most common method used for the clearance of undersea ground mines is the detonation of a large clearing charge placed either close by or in contact with the ground mine. The components of a typical ground mine that may react to the shock wave produced by the detonation of the clearing charge are the high explosive filling and the initiation train within the fuze. Depending on the stand-off distance, the shock wave may or may not initiate sympathetic detonation in the ground mine. The non-detonation events that can occur include deflagration or burning of the explosive filling, and both may be considered as unacceptable options for clearing operations.

Although the method has been in service for many years, the critical initiation parameters of an underwater shock wave and, indeed, the type of event initiated by the clearing charges, are not known. Existing theoretical [1] work describing the complex system of shock waves produced by the detonation of explosives, although definitive, is limited by the need to fit the predictions to experimental data. The various experimental studies [2,3] describing the effect of underwater shock waves on explosives are limited by the small size of the donor explosive (0.480 kg), the scope of the reaction in the acceptor (burning as compared with detonation), and the lack of suitable instrumentation to qualify the experiments. As a result of these limitations, the investigations are very restricted in assisting with the development of mine clearing procedures.

In order to assist development of operational doctrine on clearing charge deployment, Chung [4] has proposed a simple model to predict the maximum stand-off distance required for the sympathetic detonation of a ground mine. However, validation of this model requires knowledge of the shock wave's near-field peak pressure as a function of stand-off distance and the type of effect the shock wave produces when interacting with an explosive charge. Consequently, an investigation into underwater sympathetic detonation of acceptor charges, initiated by effects produced by the detonation of donor charges, was undertaken.

This report presents results describing; the type of effects resulting from shock wave-acceptor interaction, the separation distance at which this effect occurred, and the variation in near-field shock wave velocity between spherical pentolite donors and cylindrical Composition B acceptors.

# 2. Experimental Methods

## 2.1 General

The experiments were conducted in a water-filled granite quarry, 17 m deep and approximately 90 m in diameter. The site contains an instrumentation bay, two flying foxes spanning the quarry, a deployment platform and a bay suitable for charge preparation. The spherical pentolite donor charges (PETN-TNT, 50:50, density 1.64 g/cc) varied in mass from 0.5 to 10.0 kg and the Composition B acceptors (recrystallised RDX-TNT, 60:40, density 1.65 $g/cm^3$) were all 9.5 cm diameter cylinders of length 5.0, 7.5 or 15.0 cm. Both donor and acceptor charges used in the experiments were uncased. The physical dimensions of the donors and acceptors are detailed in Table 1.

The charges under test were first lowered underwater from the platform and then deployed to ground zero. The experiments were conducted approximately 8 m below the surface of the quarry, in a region free from shock wave reflections.

*Table 1. Nominal dimensions of the donor and acceptor charges used in experiments.*

| Donor Charge | | Acceptor Charge | |
|---|---|---|---|
| Nominal Mass kg | Radius cm | Nominal Mass kg | Dimensions dia×length cm |
| 0.5 | 4.17 | 0.6 | 9.5 ×5.0 |
| 2.5 | 7.13 | 0.9 | 9.5 ×7.5 |
| 5.0 | 8.98 | 1.8 | 9.5 ×15.0 |
| 10.0 | 11.31 | | |

## 2.2 Determination of Detonation of the Acceptor

It is generally agreed that shock initiation of a solid explosive produces a run-to-detonation stage during which energy is released by the growth of chemical reactions from hot-spots within the explosive [5]. The on-set of detonation occurs when the reactions become self sustaining, and cause the reaction shock wave to become stable and supersonic. Relatively long reaction times indicate that the explosive has not detonated.

The detonation of the donor charge plus the energy released during the build-up to detonation in an acceptor charge is expected to produce a complex underwater shock wave. No evidence is available to show that the far-field properties of such an underwater shock wave is suitable to determine whether the acceptor has undergone a detonation or energetic non-detonation event. Consequently, traditional methods such

as witness plates and the measurement of reaction transit time across the acceptor charge were adapted to these experiments.

## 2.3 Experimental Rig

The experimental rig in which the donor and acceptor were fixed to investigate underwater sympathetic detonation is shown in Figure 1. An array of three piezo-electric probes is taped to the end of the acceptor charge nearest the donor and a steel witness plate with a centrally positioned piezo-electric probe is attached to the rear of the acceptor. The array is used to measure the time of arrival of the shock wave incident on to the acceptor and, in conjunction with the single probe in the witness plate, to measure reaction transit time. The steel witness plate defines the type of event.

By changing the mass of the donor charge and the separation distance between the two charges, the duration and peak pressure of the underwater shock wave can be varied. As the method of deployment of the charges does not allow a final check to be made of their relative positions, they were firmly fixed in place by means of wire supports and wooden struts. Care was taken to ensure materials used in construction of the rig would not first impact on the acceptor.

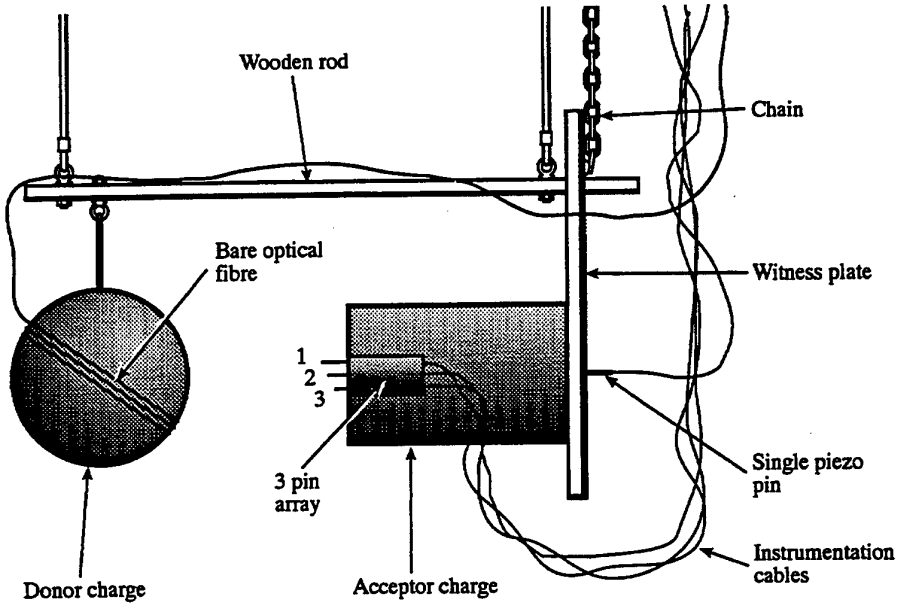


*Figure 1. Schematic of the experimental rig used for sympathetic detonation experiments.*

### 2.3.1 Witness Plates

The acceptor charge shown in Figure 1 is attached to the 6 mm thick mild steel witness plate by a circular clamp and the mass of the plate is supported by the two wooden rods of the rig. The violent reaction of the witness plate to the detonation of the acceptor is arrested by a chain welded to the plate and attached to the overhead flying fox. Seven links at each end of a 750 mm length of 10 mm diameter transport chain are laid at $45^0$ to the normal and are welded to the steel plate. Gussets are included for additional strength and are welded into place between the witness plate and high side of the chain link. The welds are optimised for strength and ductility by using CIG Autocraft 309 welding electrodes. Transport chain is looped through the welded chain and a one metre length is folded over on itself and fastened together by high tensile bolts.

Detonation of the acceptor is defined by a circular hole cleanly cut in the steel plate. Non-detonation events, such as deflagration or burning of the acceptor, are expected to produce a bulged, dented or broken plate [6].

### 2.3.2 Measurement of Incident Shock wave Velocity and Reaction Transit Time

The velocity of the incident shock wave and reaction transit time is calculated from measurements made with instrumentation shown in Figure 2. The instrumentation consists of an array of three piezo-electric probes fixed by a polycarbonate potting mix in a small plastic box, an additional piezo-electric probe positioned centrally in the witness plate, plastic fibre optical cable with an optical-electronic converter and a high resolution digital oscilloscope. The array is attached to the acceptor charge in a manner so that the bases of the probes are flush with the flat surface of the acceptor. Bare fibre optic cable is wrapped around the donor charge and the intense flash of detonation that the cable detects at the explosive-water interface is used as time zero.

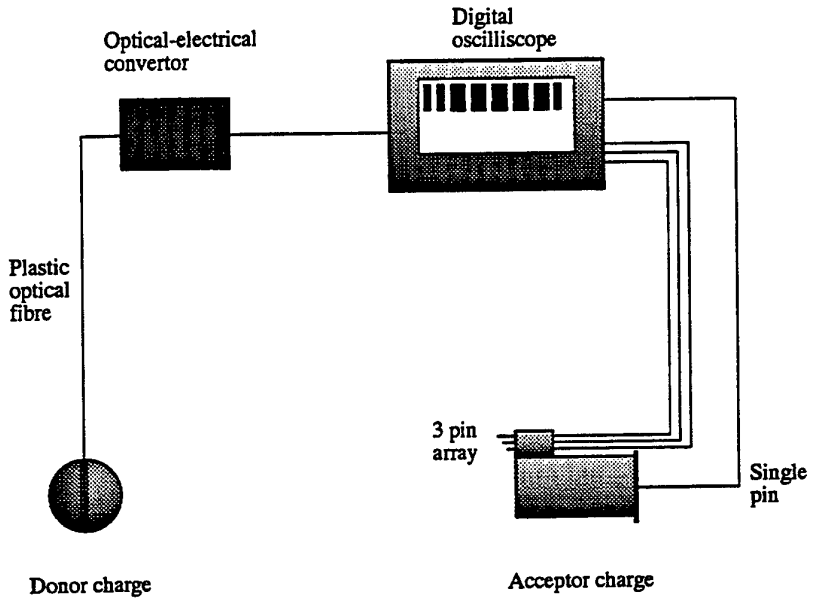


*Figure 2. Schematic of the instrumentation used to measure time of arrival of the underwater shock wave at the 3 pin array and reaction transit time of the acceptor.*

The average radial velocity $V_n$, of the incident shock wave, between the tips of the probes n and (n+1) by:

$$V_n = (X_n - X_{n+1}) / (\Delta T_n) \quad \text{n=1 or 2} \qquad (1),$$

where $X_n$ is the component of the probe length $L_n$ in the direction of motion of the shock front and $\Delta T_n$ is the time difference between the triggering of the n and (n+1) th probes.

For the geometry of the experimental rig shown in Figure 3, the component of the probe length $X_n$ in the direction of the motion of the shock front is given by:

$$X_n = L_n \cos\theta \qquad (2)$$

where θ is the angle subtended at the donor by an array of thickness 2t, attached to an acceptor cylinder of radius r, and the horizontal. The angle θ is given by:

$$\theta = \text{artan}((t+r)/(a+b)) \qquad (3),$$

when a donor of radius *a* is placed at a distance *b* from the acceptor.

Measurement of the time-of-arrival of the shock wave as it passes the tips of the probes is recorded on the oscilloscope. The average velocity between the tips of the probes can be calculated from these measurements and knowledge of the geometry of the experimental rig.

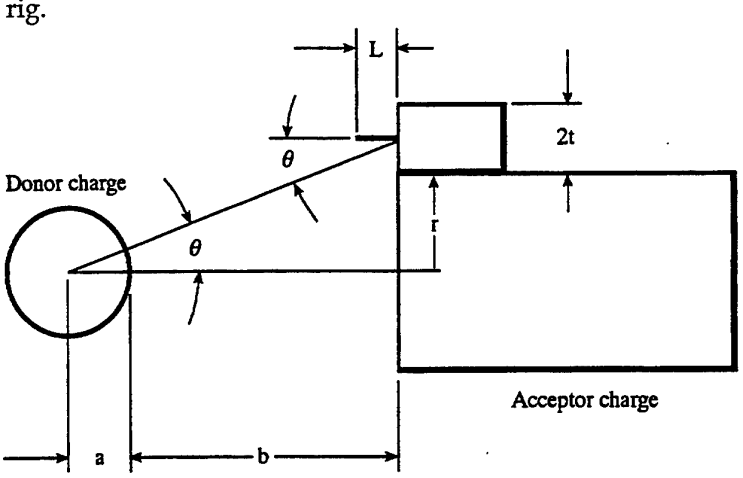


*Figure 3. Schematic of the geometry that enables the component of the pin normal to the shock front to be calculated.*

The reaction transit time $\Delta T_r$, is the time taken for the reaction wave in the acceptor to traverse its length. It may be calculated from the measurement of the time difference between the shock wave interacting with the shortest probe in the array and the reaction wave interacting with the probe positioned centrally in the witness plate $\Delta T_m$, and knowledge of the velocity of the underwater shock wave. The rig has the shortest probe fixed proud from the flat surface of the acceptor and depending on the curvature of the shock wave, the shock wave may interact with either the probe or the surface of the acceptor. For spherical waves with a large radius of curvature (i.e planar), the shock wave will first interact with the probes and the geometry describing this interaction is illustrated in Figure 4a. For positions where the donor is close to the acceptor, the radius of curvature is small and the shock wave will interact with the acceptor before the probes of the array. The geometry of this type of interaction is shown in Figure 4b.

For planar shock waves, the distance from the centre of the donor explosive to the tip of the nth probe, $h'$, is less than the distance from the centre of the donor to the flat surface of the acceptor $(a+b)$. The reaction transit time $\Delta T_r$ illustrated in Figure 4a, may be determined from:

$$\Delta T_r = \Delta T_m - \Delta T \qquad (4),$$

where $\Delta T_m$ is the measured reaction time between the two probes and $\Delta T$ is the time taken to traverse the small water gap. This transit time may be calculated from:

$$\Delta T = \left| ((a+b)-h')/V_n \right| \qquad (5),$$

where n=2 and $V_2$ is assumed to be the average velocity over the distance $(a+b)$-$h'$.

The geometry in Figures 4a and 4b show that the distance $h'$ from the centre of the donor explosive to the tip of the nth probe may be calculated from:

$$h' = h - X_n \qquad (6)$$

where the distance $h$ from the centre of the donor explosive to the base of the pin probes is shown in Figure 4 and may be expressed as:

$$h = \left[(a+b)^2 + (r+t)^2\right]^{\frac{1}{2}} \qquad (7).$$

For shock waves with a small radius of curvature, $h' > (a+b)$ and the shock wave will interact with the surface of the acceptor before the probe. The reaction transit time is illustrated in Figure 4b and may be determined from:

$$\Delta T_r = \Delta T_m + \Delta T \qquad (8).$$

The difference between the reaction transit time and the time taken for a steady detonation wave to transit the acceptor is the excess transit time and is a guide to the type of reaction that occurred in the acceptor. Small differences are indicative of a prompt detonation whilst large differences indicate a non-detonation event. The detonation velocity in Comp B is 7800 m/s [7] and for 75 and 150 mm long cylindrical acceptors, the calculated detonation transit times are 9.6 and 19.2 $\mu$s respectively.

The total time $\Delta T_t$ between time zero and the response of the single piezo-electric pin in the witness plate to the reactive shock wave is given by:

$$\Delta T_t = \Delta T_f + \Delta T_1 + \Delta T_2 + \Delta T_m \qquad (9),$$

where $\Delta T_f$ is the time for the underwater shock wave to transit the water gap between the donor and the first active piezo-electric pin in the array on the front of the acceptor.

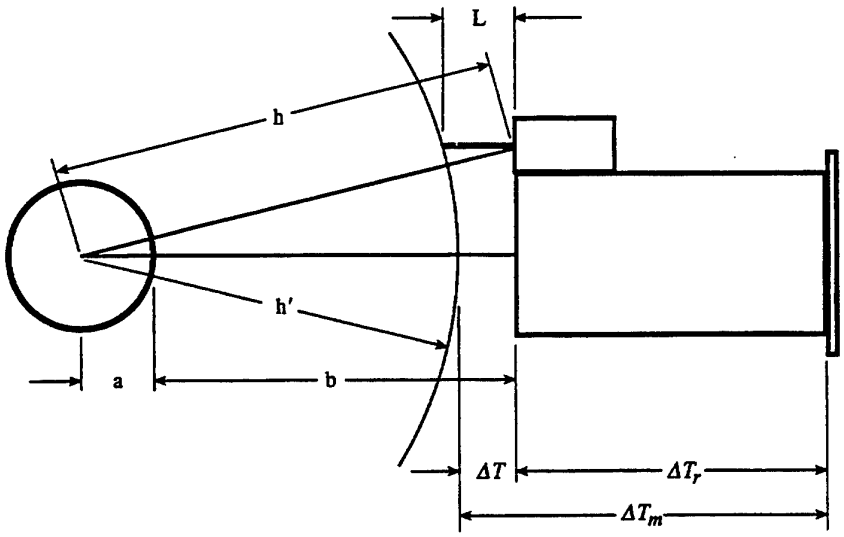


(a)

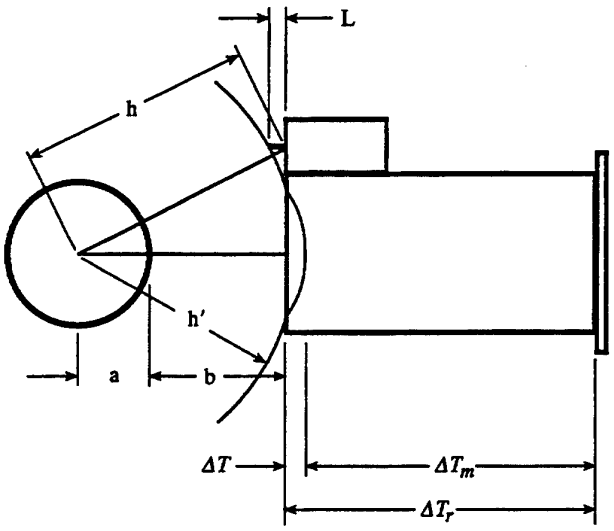


(b)

*Figure 4. Schematic showing the geometry when (a) the shock wave is planar and interacts with the probe before the acceptor and (b), a shock wave with a small radius of curvature interacting with the acceptor before the probe.*

## 2.4 Variation in Reaction Transit Time

To determine the variation in the near-field shock wave velocity with separation, the mass of the donor and distance between donor and acceptor is varied. This varies the magnitude of the peak pressure at the water/explosive interface and hence the pressure and the velocity $V_s$ of the reaction shock wave within the acceptor. If the reaction wave initiates detonation within the acceptor, its velocity will determine the run-to-detonation distance $d$ and thus the reaction transit time $T_r$. The transition from reaction shock wave to detonation wave is not abrupt [5] and, for simplicity, the series of events are shown in Figure 5.

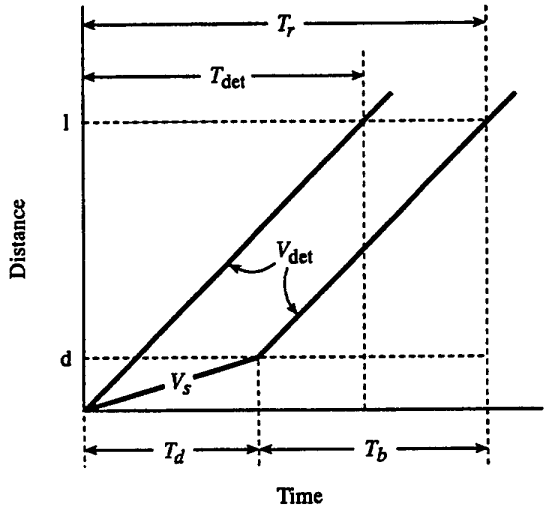


*Figure 5. Schematic of a space-time plot of shock initiation of acceptor charges, l cm long.*

Here, the reaction shock wave takes $T_d$ seconds to transit the run-to-detonation distance and the detonation wave takes $Tb$ seconds to transit the remainder of the acceptor. The reaction transit time may be expressed as:

$$T_r = T_d + T_b \qquad (10).$$

If $T_{det}$ is the time taken for the detonation wave of velocity $V_{det}$ to transit the acceptor of length $l$, then the excess transit time $T_e$, may be expressed as:

$$T_e = T_r - T_{det} \qquad (11).$$

Substituting the reaction transit time from equation (10) into equation (11) gives:

$$T_e = T_d + T_b - T_{det} \qquad (12).$$

The ratio of excess transit time to detonation transit time enables the measured transit times to be expressed in terms of detonation transit times. Therefore, normalising the excess transit times with respect to the detonation transit time gives:

$$\text{Nrt} = \frac{T_e}{T_{\text{det}}} = \frac{T_d + T_b}{T_{\text{det}}} - 1 \qquad (13)$$

and substituting $T_d = \frac{d}{V_s}$, $T_b = \frac{d-l}{V_{\text{det}}}$ and $T_{\text{det}} = \frac{l}{V_{\text{det}}}$ allows Nrt to be obtained in the form:

$$\text{Nrt} = \frac{d}{l}\left[\frac{V_{\text{det}}}{V_s} - 1\right] \qquad (14).$$

When $d \cong 0$, detonation would occur at the face of the acceptor charge and $V_s \cong V_{\text{det}}$. Equation (14) shows Nrt=0.

When $d = l$, detonation would occur at the end of the acceptor, indicating that the reaction shock wave requires a long run-to-detonation distance and implies that $V_s << V_{\text{det}}$. It is improbable that detonation would be initiated under these conditions and equation (14) shows that Nrt>>1, how much greater than 1, it is not clear.

For values of $d$ intermediate to the above extremes and for values of $\frac{V_{\text{det}}}{V_s}$ ranging from 2 to 3, equation (14) shows that Nrt ranges from 0.25 to 1.5.

# 3. Results

Four series of tests were carried out to determine the maximum separation distance required to initiate sympathetic detonation in cylindrical Comp B charges by the detonation of spherical pentolite donors. The maximum separation distances and the results, determined by effects on the witness plates, for donor masses of 0.5, 2.5, 5.0, and 10.0 kg are listed in Table 2. The probe lengths, arrival times of the shock waves and reaction transit times where available, are also listed in Table 2.

*Table 2. Charge masses, separation distances, probe lengths, arrival times, reaction transit times and effects determined by witness plates for sympathetic detonation of Comp B acceptors by detonating pentolite donors.*

| Test | Donor Mass, M kg | Acceptor Mass kg | Separation Distance cm | L1 cm | L2 cm | L3 cm | ΔT1 μs | ΔT2 μs | ΔTm μs | Result |
|---|---|---|---|---|---|---|---|---|---|---|
| | | | | | | | Not Recorded | | | |
| 1 | 0.5 | 0.6 | 3 | | | | .. | .. | .. | D |
| 2 | 0.5 | 0.6 | 6 | | | | .. | .. | .. | D |
| 3 | 0.5 | 0.6 | 12 | | | | .. | .. | .. | ND |
| 4 | 0.5 | 0.6 | 6 | | | | .. | .. | .. | D |
| 5 | 0.5 | 0.6 | 9 | | | | .. | .. | .. | ND |
| 6 | 0.5 | 0.6 | 6 | | | | .. | .. | .. | D |
| 7 | 0.5 | 0.6 | 9 | | | | .. | .. | .. | ND |
| | | | | | | | .. | .. | .. | |
| 8 | 2.5 | 0.6 | 4 | | | | .. | .. | .. | D |
| 9 | 2.5 | 0.6 | 9 | | | | .. | .. | .. | D? |
| 10 | 2.5 | 0.9 | 9 | | | | .. | .. | 8.24 | D |
| 11 | 2.5 | 1.8 | 9 | 2.2 | 1.2 | 0.22 | 2.92 | 3.48 | 29.04 | D |
| 12 | 2.5 | 1.8 | 11.5 | 2.2 | 1.2 | 0.24 | 3.72 | 4.08 | 36.48 | D |
| 13 | 2.5 | 1.8 | 14 | 2.21 | 1.27 | 0.23 | 4.24 | 5.0 | 46.28 | ND |
| 14 | 2.5 | 1.8 | 11.5 | 2.22 | 1.21 | 0.20 | 3.36 | 3.96 | 36.36 | D |
| 15 | 2.5 | 1.8 | 14 | 2.14 | 1.17 | 0.23 | Not Recorded | | | ND |
| 16 | 2.5 | 1.8 | 11.5 | 2.21 | 1.20 | 0.25 | 3.84 | 4.36 | 30.36 | D |
| 17 | 5 | 0.9 | 4 | | | | N R | N R | N R | D |
| 18 | 5 | 0.9 | 9 | | | | .. | .. | .. | ND |
| 19 | 5 | 0.9 | 12 | 2.22 | 1.22 | 0.20 | 8.60 | N R | 14.76 | D |
| 20 | 5 | 0.9 | 9 | 2.21 | 1.23 | 0.28 | 8.02 | N R | 13.18 | D |
| 21 | 5 | 1.8 | 9 | 2.21 | 1.21 | 0.21 | N R | 4.12 | 17.24 | D |
| 22 | 5 | 1.8 | 12 | 2.23 | 1.24 | 0.31 | .. | 3.28 | N R | D |
| 23 | 5 | 1.8 | 15 | 2.21 | 1.20 | 0.22 | .. | 3.88 | 25.40 | D |
| 24 | 5 | 1.8 | 18 | 2.20 | 1.22 | 0.22 | .. | 3.48 | 31.48 | D |
| 25 | 5 | 1.8 | 21 | 2.23 | 1.23 | 0.28 | .. | 3.72 | N R | ND |
| 26 | 5 | 1.8 | 18 | 2.23 | 1.22 | 0.24 | .. | 4.68 | 31.92 | D |
| 27 | 5 | 1.8 | 21 | 2.20 | 1.20 | 0.25 | 4.36 | 4.60 | 54.24 | ND |
| 28 | 5 | 1.8 | 18 | 2.22 | 1.24 | 0.24 | 3.92 | 4.48 | 41.84 | D |
| 29 | 10 | 0.9 | 12 | 2.26 | 1.30 | 0.28 | 6.44 | N R | 11.16 | D |
| 30 | 10 | 1.8 | 22 | 2.20 | 1.22 | 0.22 | 3.36 | 3.72 | 29.68 | D |
| 31 | 10 | 1.8 | 25 | 2.18 | 1.20 | 0.25 | 4.20 | 4.40 | 45.32 | D |
| 32 | 10 | 1.8 | 28 | 2.18 | 1.17 | 0.23 | 4.68 | 4.52 | 56.00 | ND |
| 33 | 10 | 1.8 | 25 | 2.23 | 1.25 | 0.23 | 3.56 | 4.04 | 39.50 | D |
| 34 | 10 | 1.8 | 28 | 2.17 | 1.22 | 0.23 | 4.28 | 4.56 | 57.12 | ND |
| 35 | 10 | 1.8 | 25 | 2.03 | 1.25 | 0.22 | 3.44 | 4.80 | 36.60 | D |

D - Detonation ND - Non-Detonation N R - Not Recorded

The pins did not record results during some events either because of the failure of the triggering pulse or the reallocation of an instrumentation cable for far-field measurements. The triggering problem was overcome by using pin 1 of the array to trigger instrumentation during events 21 to 26. The result for event 19 was determined from the excess transit time.

The water gap transit times $\Delta T_f$ for selected donor masses and separations were measured and are shown in Table 3. The total time $\Delta T_t$ was calculated from equation (9). These results and estimations [8] of the times taken for the bubble containing detonation products to expand to the front surface of the acceptor charge are also shown in Table 3.

*Table 3. A comparison of the times for a shock wave to transit, and bubble to expand over, similar distances.*

| Test | $\Delta T_f$ | $\Delta T_t$ | Bubble expansion time |
|---|---|---|---|
| | $\mu$s | $\mu$s | $\mu$s |
| 10 | 13.2 | 21.4 | 317 |
| 20 | 24.2 | 32.2 | 404 |
| 29 | 27.96 | 45.6 | 810 |

The Bruceton statistical technique [9] was used to determine the surface-to-surface separation between the explosives for 50% probability of acceptor detonation, and separations corresponding to the 5% and 95% probability were also calculated. These results are shown in Table 4.

*Table 4. Statistically determined distances for underwater sympathetic detonation of cylindrical Comp B acceptors by detonation of spherical Pentolite donors.*

| **Donor Mass, M kg** | **Separation Distance for Sympathetic Detonation of Comp B Acceptor, cm** | | |
|---|---|---|---|
| | **Probability of Detonation** | | |
| | **5%** | **50%** | **95%** |
| 0.5 | 10.8 | 7.5 | 4.2 |
| 2.5 | 16.7 | 12.8 | 8.9 |
| 5.0 | 22.5 | 19.5 | 16.1 |
| 10.0 | 29.8 | 26.5 | 23.1 |

The probe lengths were modified using equations (1) and (2) for t=1.5 cm and r=4.75 cm. The incident shock wave velocity was calculated from equation (1) for all results in Table 2. To enable the shock wave velocities from various charges to be plotted on the same set of axis, the separation distance between donor and acceptor was made proportional to the reduced separation distance, $b/M^{0.3}$. The effect shock wave velocity has on the initiation of detonation in the acceptor is shown in Figures 6a and 6b.

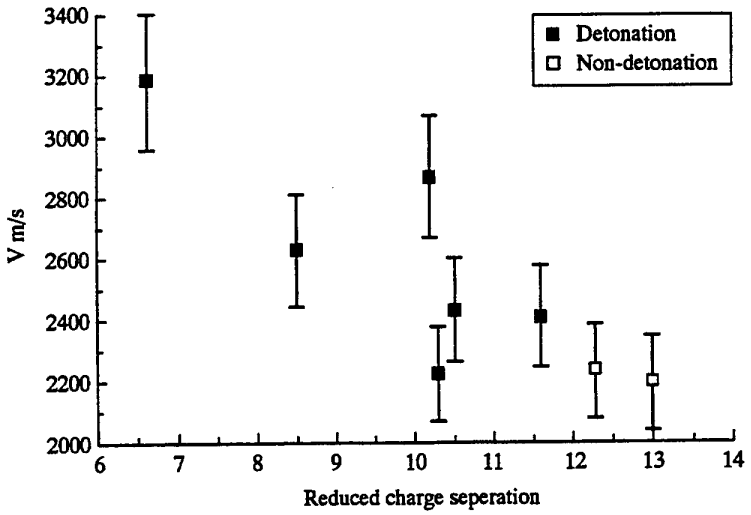


*Figure 6a. Average velocity of underwater shock waves, measured by pins L1 and L2, versus reduced charge separation for detonation and non-detonation events.*

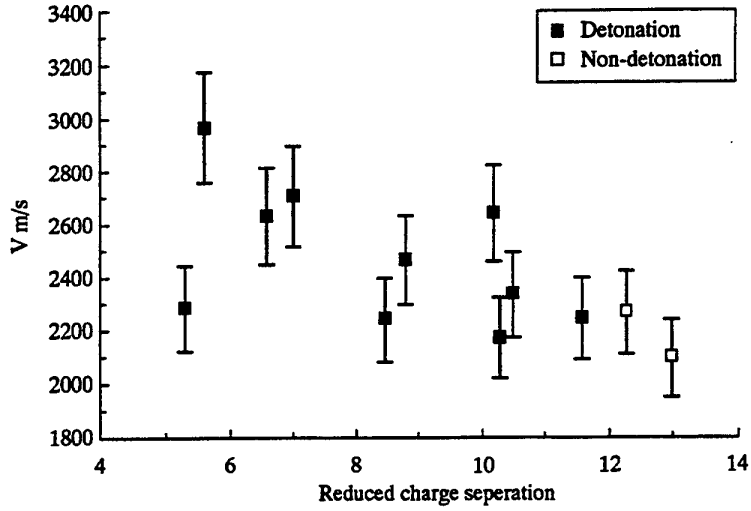


*Figure 6b. Average velocity of underwater shock waves, measured by pins L2 and L3, versus reduced charge separation for detonation and non-detonation events.*

Neglecting the scatter of experimental results, a power curve of best fit to the set of results measured by the two piezo-electric pins, L1 and L2 and shown in Figure 6a, is given by:

$$V = \frac{8294}{R^{0.52}} \qquad (15),$$

where $V$ is the average shock wave velocity in m/s and $R$ is the reduced distance measured from the surface of the donor charge. A similar curve fitted to the results shown in Figure 6b, measured by the two piezo-electric pins, L2 and L3 approximately 1 cm closer to the surface of the acceptor, gives the velocity of the shock wave as:

$$V = \frac{5330}{R^{0.35}} \qquad (16).$$

The coefficients of determination for equations (15) and (16) are 0.96 and 0.87 respectively.

Corrections to reaction transit times due to the curvature of the shock wave were made from the velocity model developed from Figures 6 and equations (4), (5) and (8). The results are shown in Table 5, together with the effects determined by witness plates. The excess transit times and the ratio of the excess reaction transit time to the detonation transit time, Nrt, for each event are also included in this Table.

*Table 5. Transit times of a reactive shock wave passing through Comp B acceptors. The detonation transit times for 95×75 and 95×150 mm acceptors are 9.6 and 19.2 us respectively.*

| Test | Measured Transit Time $\mu$s | Curvature correction $\mu$s | Corrected Transit Time $\mu$s | Excess Transit Time $\mu$s | Nrt | Result from witness plate |
|---|---|---|---|---|---|---|
| 1 | not recorded | | | | | D |
| 2 | .. | | | | | D |
| 3 | .. | | | | | ND |
| 4 | .. | | | | | D |
| 5 | .. | | | | | ND |
| 6 | .. | | | | | D |
| 7 | .. | | | | | ND |
| 8 | .. | | | | | D |
| 9 | .. | | | | | D |
| 10 | 8.24 | 2.6 | 10.84 | 1.64 | 0.18 | D |
| 11 | 29.04 | 3.5 | 32.54 | 13.34 | 0.69 | D |

*Table 5. (continued) Transit times of a reactive shock wave passing through Comp B acceptors. The detonation transit times for 95×75 and 95×150 mm acceptors are 9.6 and 19.2 us respectively.*

| Test | Measured Transit Time $\mu s$ | Curvature correction $\mu s$ | Corrected Transit Time $\mu s$ | Excess Transit Time $\mu s$ | Nrt | Result from witness plate |
|---|---|---|---|---|---|---|
| 12 | 36.48 | 3.1 | 39.58 | 20.38 | 1.06 | D |
| 13 | 46.28 | 3.0 | 49.48 | 30.28 | 1.58 | ND |
| 14 | 36.36 | 3.2 | 39.56 | 20.36 | 1.06 | D |
| 15 | not recorded | | | | | ND |
| 16 | 30.36 | 3.1 | 33.46 | 14.26 | 0.74 | D |
| 17 | not recorded | | | | | D |
| 18 | .. | | | | | ND |
| 19 | 14.76 | 2.6 | 17.36 | 7.76 | 0.81 | ND |
| 20 | 13.18 | 2.6 | 15.78 | 6.18 | 0.64 | D |
| 21 | 17.24 | 2.8 | 20.04 | 8.4 | 0.44 | D |
| 22 | not recorded | | | | | D |
| 23 | 25.40 | 2.4 | 27.8 | 8.6 | 0.45 | D |
| 24 | 31.48 | 2.2 | 33.68 | 14.48 | 0.75 | D |
| 25 | not recorded | | | | | ND |
| 26 | 31.92 | 2.1 | 33.92 | 14.72 | 0.77 | D |
| 27 | 54.24 | 1.8 | 56.04 | 36.84 | 1.92 | ND |
| 28 | 41.48 | 2.1 | 43.58 | 24.38 | 1.27 | D |
| 29 | 11.16 | 2.0 | 13.16 | 3.56 | 0.37 | D |
| 30 | 29.68 | 2.0 | 31.68 | 12.48 | 0.65 | D |
| 31 | 45.32 | 1.4 | 46.72 | 27.52 | 1.43 | D |
| 32 | 56.00 | 1.3 | 57.3 | 38.10 | 1.98 | ND |
| 33 | 39.50 | 1.5 | 41.0 | 21.8 | 1.14 | D |
| 34 | 57.12 | 1.3 | 58.42 | 39.22 | 2.04 | ND |
| 35 | 36.60 | 1.5 | 38.10 | 18.90 | 0.98 | D |

D - Detonation ND - Non-Detonation

One or more of the variables; corrected transit time, excess transit time or Nrt, may assist in the determination of underwater sympathetic detonation. These variables were plotted independently against charge separation and are shown in Figures 7, 8 and 9 respectively.

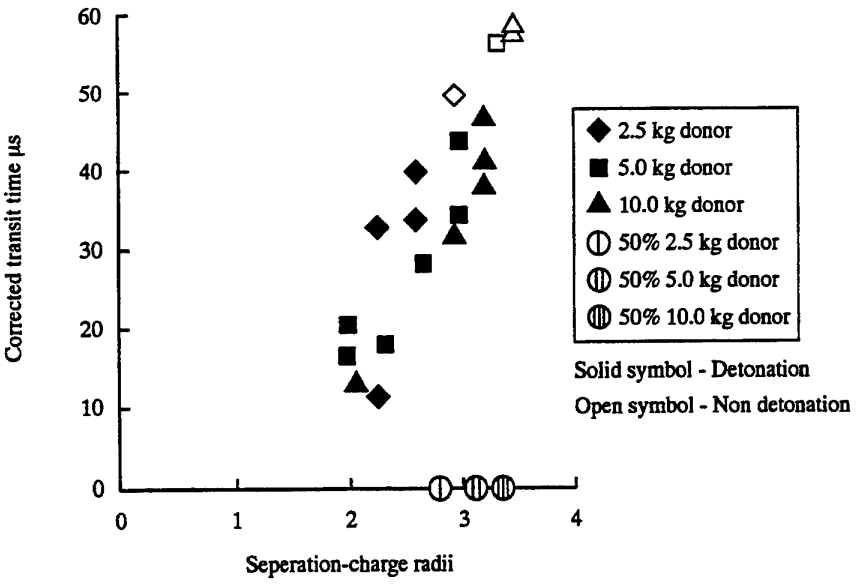


*Figure 7. Corrected transit time versus charge separation. The separations for 50% probability of detonation are shown on the X axis. The radius of the donor charge is also included in the separation distance.*

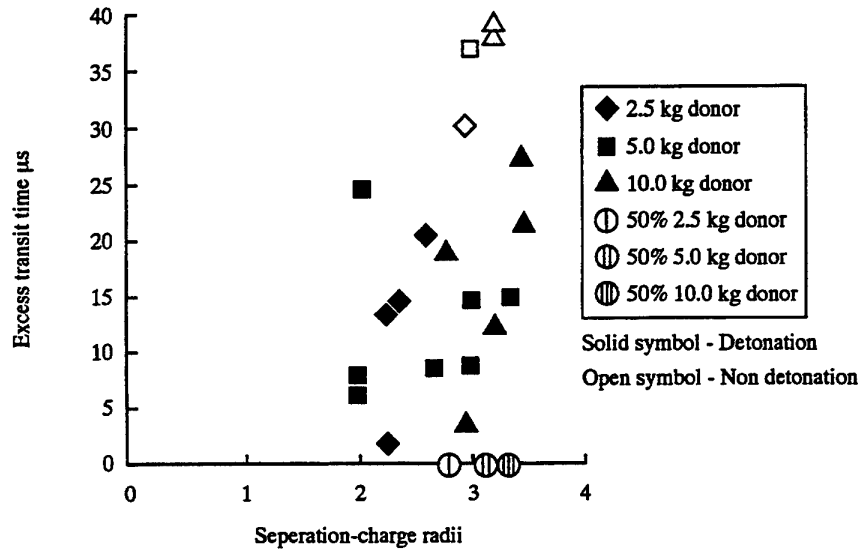


*Figure 8. Excess transit time versus separation distance. The separation for 50% probability of detonation is shown on the X axis. The radius of the donor charge is included in the separation distance.*

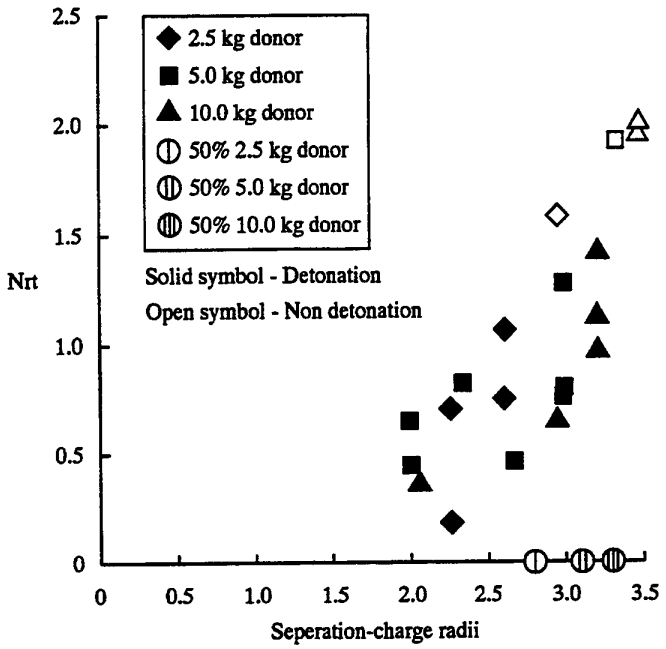


*Figure 9. Normalised excess transit times versus charge separation. The separations for 50% probability of detonation is shown on the X axis. The radius of the donor charge is also included in the separation distance.*

# 4. Discussion

The separation between donor and acceptor for the initial event of each series of experiments was small. This ensured the acceptor charge sympathetically detonated and enabled sympathetic detonation effects to be characterised by the witness plate and the support instrumentation.

The steel witness plates proved a most reliable method to determine detonation or non-detonation of the Composition B acceptors. However, from observation of the damage sustained by the plates, clearly several types of events occurred during the course of the experiments. A circular hole cleanly cut in the witness plates confirmed that detonation in the acceptor had been established, whilst witness plates that were ripped, twisted and retained part of the circular disk, indicated that a violent non-detonation event had occurred. Other plates were simply dished. The various damage levels of the witness plates cannot be reliably related to the type of non-detonation reaction occurring in the acceptor, therefore the last two effects have been defined in Table 2 as non-detonation events.

From a comparison of $\Delta T_i$ and the estimation of the bubble expansion times in Table 3, we are sure that the underwater shock wave has reacted with the acceptor charge long before the bubble has reached the acceptor. Subsequent experiments [10] using a high

speed cine-camera in a small scale underwater test facility confirmed that the reaction in the acceptor is initiated by the shock wave alone.

The increments in the spacings used for the Bruceton method, although large, were within two standard deviations as required by the technique [9]. These large steps were used to quickly straddle the 50% probability of detonation separation distance for each donor. The results from the Bruceton test are shown in Table 4 and can be used as a basis for additional testing if a greater confidence in calculating probability separations is required.

The maximum percentage error in the shock wave velocity is estimated to be 7%. This percentage error was determined from the spread in the velocities averaged at particular reduced charge separations and is greater than errors accumulated in measurement of the pin length and the time-of-arrival of the shock wave (3%). The donor and acceptor charges were fixed by means of wooden rods and wire prior to deployment. However, we suspect that there will be some movement between the two charges on deployment and the maximum percentage error due to this movement was estimated to be 5%.

The sympathetic detonation experiments were conducted at separations ranging from 2 to 4 charge radii that are regions typically achievable during mine clearing operations. The shock wave velocities calculated in these experiments vary from 2000 to 3200 m/s which are far greater than acoustic velocities (approx.1488 m/s). Duvall and Fowles [10] have shown that the pressure of a shock wave traversing a medium is a function of the density of the unshocked medium, the shock wave velocity and the velocity of the particles associated with the shock wave. Thus, the pressure of a shock wave in regions typical of mine clearing operations will be greater than those pressures determined at acoustic velocities.

Power curves were found to be the curves of best fit to describe the data presented in Figures 6a and 6b. The greater coefficient of determination (0.95) indicates that equation (15) is a better fit to the data and should be used to model the velocity in the near fields. However, the scatter and limited amount of data available to model the variation in shock wave velocity with distance suggests further investigations are advisable. Expressing the shock velocity in terms of reduced charge separation provides a means by which equation (15) can be simply applied to underwater charges of different scale. The data in Figures 6a and 6b indicate that the shock wave velocity rapidly reduces with distance from the centre of detonation. We expect that the shock wave velocity will approach the acoustic velocity which is 1488 m/s for the conditions within the quarry. The onset of this velocity occurs in the far-field of the detonated donor charge and equation (15) suggests that this region begins at separations greater than 5.2 charge radii from the centre of the donor charge.

The corrections in transit times due to the curvature of the shock wave are shown in Table 5 and although small, they were included in the calculation of excess transit times. Run-to-detonation distances in the acceptors were estimated from equation (15),

impedance matching techniques and excess transit times [5]. These distances were found to range from 3.5 to 11.0 cm and the estimation is supported by high speed cine recordings made under similar experimental conditions in a small scale test facility [11]. Measurements from these experiments have shown that detonation break-out occurs 5 cm into the acceptor.

The corrected transit times for all acceptors plotted in Figure 7 follow a similar trend. These times increase with increase in separation until a point is reached where there occurs a large increase in transit time for a small or no increase in separation, producing a 'step' in the data. Beyond this point, the increase in transit time slows with increase in separation. This trend can be explained in terms of reduction in peak pressure. As the separation is increased, the peak pressure at the water/charge interface decreases which in turn decreases the pressure in the acceptor and hence the velocity of the reaction wave within the acceptor charge. Slower reaction waves are expected to initiate detonation deeper in the acceptor and take a longer time to transit the acceptor charge. A lower limit in the velocity of the reaction wave will eventually be reached, below which detonation will not be initiated.

The experimental results show that detonation occurred in the acceptors for transit times up to and including those values contained in the step. The experimental results also show that non-detonation occurred for values of transit times beyond the step. The steps in the data are seen to correspond very closely to the 50% probability of detonation separations for 2.5, 5.0 and 10.0 kg acceptors that are plotted at 2.8, 3.1 and 3.3 charge radii respectively. The transit time step for these experiments occurs over a range of 35-45 $\mu s$. However, this range cannot be used as a guide for experiments with other explosives because transit times are dependant on the length and density of the explosive material in the acceptor.

The results for excess transit times plotted against charge separation for the same experiments are shown scattered in Figure 8. They show no distinctive trend for any donor charge although non-detonation events are seen to occur for excess transit times greater than 30 $\mu s$. However, this time is also dependant on the length and density of the acceptor charge and could not be confidently extended to other explosive materials.

The normalised excess transit time ratio Nrt, versus charge separation for each event is shown in Figure 9. The trends in these results are similar to those for the corrected transit time curves shown in Figure 7, and in addition, the values of Nrt for detonation and non-detonation of the acceptor charge fall into ranges deduced in Section 2.4. Here, detonation occurs for the values of Nrt ranging from zero to 1.5 and for Nrt > 1.5 non-detonation occurs.

The data in Figure 9 is independent of the length and density of the acceptor charge and may provide a method to determine the on-set of sympathetic detonation in Composition B acceptors during underwater field experiments. The data shows that when the excess transit time equals or is 1.5 times the detonation transit time,

detonation has been initiated in the acceptors. This method may also prove a useful guide for other explosive materials.

# 5. Conclusion

The results from these experiments have given a better understanding of the effects of underwater blast on Composition B in regions close by an exploding spherical, pentolite charge. We have developed techniques that will allow us to predict the peak pressure of the shock wave in the water between the donor and acceptor from which, predictions of the pressure within the explosive acceptor will follow. These techniques will allow us to investigate the critical initiation parameters of an underwater shock wave and ultimately, to assist in the development of mine clearing techniques.

Witness plates have proved a reliable method of determining the type of effect that results from the interaction of an underwater shock wave with a Composition B acceptor. The varying levels of damage sustained by the witness plates indicate that three different types of reaction occurred in the acceptor charge. However, insufficient data prevented these non-detonation events from being analysed to determine if there are separations that may lead to other, less energetic methods of mine neutralisation.

A comparison of shock wave arrival times and bubble expansion times indicate that the reaction in the Composition B acceptor charge was initiated by the underwater shock wave alone.

The Bruceton technique has determined separations for the 50% probability of sympathetic detonation of a Composition B acceptor by four different masses of donor charge. The threshold separations are in good agreement with the large increase in normalised excess transit times.

The velocity of a shock wave at distances less than 5.2 charge radii from a detonating charge is much greater than the acoustic velocity. In these regions, the peak pressure is dependant on the velocity of the shock wave, resulting in a peak pressure that is greater than that of a shock wave propagating at acoustic velocities.

Excess transit times, normalised to the detonation transit time are independent of charge length and can be used as a guide to determine detonation and non-detonation events. However, from the small sample of data available, they cannot discern the types of non-detonation events that are reflected by the damage sustained by the witness plates.

# 6. Acknowledgments

This paper is the result of the efforts from several field trials. We should like to thank staff from Specialised Instrumentation SSMD, in particular; Messrs G. Yiannakopoulos, A. Pleckauskas and A. Krelle for their technical assistance and Messrs M. Chick and M. Wolfson for their advice during these trials.

# 7. References

1. Sternberg, H.M., Walker, W.A., (Sept. 1971) Calculated Flow and Energy Distribution Following Underwater Detonation of a Pentolite Sphere. The Physics of Fluids. Vol. 14, No. 9, pp 1869-1878.
2. Liddiard, T.P., Forbes, J.W., (March 1987) A Summary Report of the Modified Gap Test and the Underwater Sensitivity Test. Naval Surface Warfare Centre, Dahlgren.
3. Nailer, D.N., (1979) Joint US/UK Mine Destruction Trials-Sympathetic Detonation Element, AUWE Publication 47757, Portland, UK. Confidential.
4. Chung, M.J., (1993) A Review on Underwater Sympathetic Detonation of Ground Mines. MRL-TR-93-52, Aeronautical and Maritime Research Laboratory, Melbourne.
5. Ramsay, J.B., Popolato, A., (1965) Analysis of Shock Wave and Initiation Data for Solid Explosives. Fourth Symp. on Detonation, U.S. Naval Ordnance Laboratory, White Oak, Maryland.
6. Wolfson, M.G., (1993). A Large Scale Gap Test at MRL for Measuring Shock Sensitivity of Explosive Fillings for Insensitive Munitions. MRL-TR-93-43, Aeronautical and Maritime Research Laboratory, Melbourne.
7. Price, D., Clairmont Jr., A.R., Erkman, J.O., (1974) The NOL Large Scale Gap Test.III. Compilation of Unclassified Data and Supplementary Information of Results. Naval Ordnance Laboratory, White Oak, Maryland.
8. Cole, R.H., (1948). Underwater Explosions. Princeton University Press, New Jersey.
9. Dixon, W.J, Mood, A.M., A Method for Obtaining and Analyzing Sensitivity Data. American Statistical Society.
10. Duvall, G.F., Fowles, R. (1963). Chapter 9, Shock Waves, ed. Bradley, R.S., Academic Press, London.
11. Chung, M.J., Kinsey, T , (1994). A Study of Underwater Blast Effects on Simple Structures, Shielded and Bare Explosive Materials. Accepted by the 4th Int. Sym. on Behaviour of Dense Media Under High Dynamic Pressures. France.

DISTRIBUTION LIST

Initiation of Detonation in Composition B by an Underwater Shock Wave

Michael Chung, Darren McQueen and Lyn McVay

**AUSTRALIA**

**DEFENCE ORGANISATION**

**Task sponsor** DNW

**S&T Program**

Chief Defence Scientist
FAS Science Policy
AS Science Industry and External Relations
AS Science Corporate Management
} shared copy

Counsellor Defence Science, London (Doc Data Sheet)
Counsellor Defence Science, Washington (Doc Data Sheet)
Senior Defence Scientific Adviser/Scientific Adviser Policy and Command (shared copy)
Navy Scientific Adviser
Scientific Adviser - Army (Doc Data Sheet and distribution list only)
Air Force Scientific Adviser
Director Trials

**Aeronautical and Maritime Research Laboratory**

Director
Chief, Weapons Systems Division
D. Thompson
M. Chick
M. Chung
D. McQueen
L. McVay

**Electronics and Surveillance Laboratory**

Director

**DSTO Library**

Library Fishermens Bend
Library Maribyrnong
Library DSTOS ( 2 copies)
Library, MOD, Pyrmont (Doc Data sheet only)
Australian Archives

**Forces Executive**

Director General Force Development (Sea)
Director General Force Development (Land) (Doc Data Sheet only)
Director General Force Development (Air) (Doc Data Sheet only)

**Navy**

SO (Science), Director of Naval Warfare, Maritime Headquarters Annex, Garden Island, NSW 2000 (Doc Data Sheet only)
MHC Project Director, CP2-3-14, Canberra ACT
MWSC Project Director, CP2-2-19, Canberra ACT

**Army**

ABCA Office, G-1-34, Russell Offices, Canberra (4 copies)

**S&I Program**

Defence Intelligence Organisation
Library, Defence Signals Directorate (Doc Data Sheet only)

**B&M Program (libraries)**

OIC TRS, Defence Central Library
Officer in Charge, Document Exchange Centre (DEC), 1 copy
*US Defence Technical Information Centre, 2 copies
*UK Defence Research Information Centre, 2 copies
*Canada Defence Scientific Information Service, 1 copy
*NZ Defence Information Centre, 1 copy
National Library of Australia, 1 copy

**UNIVERSITIES AND COLLEGES**

Australian Defence Force Academy
Library
Head of Aerospace and Mechanical Engineering
Deakin University, Serials Section (M list), Deakin University Library, Geelong, 3217
Senior Librarian, Hargrave Library, Monash University
Librarian, Flinders University

**OTHER ORGANISATIONS**

NASA (Canberra)
AGPS

**OUTSIDE AUSTRALIA**

**ABSTRACTING AND INFORMATION ORGANISATIONS**

INSPEC: Acquisitions Section Institution of Electrical Engineers
Library, Chemical Abstracts Reference Service
Engineering Societies Library, US
American Society for Metals
Documents Librarian, The Center for Research Libraries, US

**INFORMATION EXCHANGE AGREEMENT PARTNERS**

Acquisitions Unit, Science Reference and Information Service, UK
Library - Exchange Desk, National Institute of Standards and Technology, US

SPARES (10 copies)

**Total number of copies: 57**

**DEFENCE SCIENCE AND TECHNOLOGY ORGANISATION**
**DOCUMENT CONTROL DATA**

1. PRIVACY MARKING/CAVEAT (OF DOCUMENT)

2. TITLE

Initiation of Detonation in Composition B by an Underwater Shock Wave

3. SECURITY CLASSIFICATION (FOR UNCLASSIFIED REPORTS THAT ARE LIMITED RELEASE USE (L) NEXT TO DOCUMENT CLASSIFICATION)

| | |
|---|---|
| Document | (U) |
| Title | (U) |
| Abstract | (U) |

4. AUTHOR(S)

Michael Chung, Darren McQueen and Lyn McVay

5. CORPORATE AUTHOR

Aeronautical and Maritime Research Laboratory
PO Box 4331
Melbourne Vic 3001

| 6a. DSTO NUMBER | 6b. AR NUMBER | 6c. TYPE OF REPORT | 7. DOCUMENT DATE |
|---|---|---|---|
| DSTO-TR-0273 | AR-009-426 | Technical Report | September 1996 |

| 8. FILE NUMBER | 9. TASK NUMBER | 10. TASK SPONSOR | 11. NO. OF PAGES | 12. NO. OF REFERENCES |
|---|---|---|---|---|
| G6/4/8-4705 | NAV 91/167 | DNW | 21 | 11 |

13. DOWNGRADING/DELIMITING INSTRUCTIONS

None

14. RELEASE AUTHORITY

Chief, Weapons Systems Division

15. SECONDARY RELEASE STATEMENT OF THIS DOCUMENT

*Approved for public release*

OVERSEAS ENQUIRIES OUTSIDE STATED LIMITATIONS SHOULD BE REFERRED THROUGH DOCUMENT EXCHANGE CENTRE, DIS NETWORK OFFICE, DEPT OF DEFENCE, CAMPBELL PARK OFFICES, CANBERRA ACT 2600

16. DELIBERATE ANNOUNCEMENT

No limitations

17. CASUAL ANNOUNCEMENT Yes

18. DEFTEST DESCRIPTORS

Detonation, Initiation, Composition and explosives, Shock waves, Underwater explosives

19. ABSTRACT

This paper examines the interaction of underwater shock waves with bare, cylindrical Composition B acceptor charges. Suitable methods to discern detonation and non-detonation of an underwater charge were determined. Separation distances for the 50% probability of sympathetic detonation of Composition B acceptors using 0.5, 2.5, 5.0 and 10.0 kg spherical pentolite donor charges were calculated from the Bruceton technique. The variation in near-field shock wave velocity between donor and acceptor charges was modelled in terms of reduced charge separation to permit an economy of effort in predictions of the effects from underwater charges of a changed scale. Measurement of shock wave transit times indicate that initiation of detonation in the acceptor is due to the underwater shock wave alone.